

CHEMISTRY 
A EUROPEAN JOURNAL

Supporting Information

© Copyright Wiley-VCH Verlag GmbH & Co. KGaA, 69451 Weinheim, 2008

Reaching Optimal Light-Induced Intramolecular Spin Alignment within Photo-Magnetic Molecular Device Prototypes

Ilaria Ciofini,^{*,[a]} Carlo Adamo,^[a] Yoshio Teki,^[b] Fabien Tuyères,^[c] and Philippe P. Lainé^{*,[c]}

*[a] Laboratoire d'Électrochimie et Chimie Analytique (CNRS UMR-7575)
École Nationale Supérieure de Chimie de Paris
11, rue Pierre et Marie Curie, F-75231 Paris Cedex 05 (France)*

*[b] Department of Material Science
Graduate School of Science, Osaka City University
3-3-138 Sugimoto, Sumiyoshi-ku, Osaka 558-8585 (Japan)*

*[c] Laboratoire de Chimie et Biochimie Pharmacologiques et Toxicologiques (CNRS UMR-8601)
Université Paris Descartes
Faculté de Médecine, 45, rue des Saints Pères, F-75270 Paris Cedex 06 (France)*

Table SI-I. Selected structural parameters computed for imino-nitroxide (IN) derivatives in the ground (**Td5**, **Dd5**, **Td6**, **Dd6**) and in the excited state (**Td5***, **Dd5***, **Td6***, **Dd6***) as a function of the overall spin state, and in comparison with available X-ray data. Distances in Å, angles in degrees. For labeling scheme refer to Figures 1, 2 and 3.

	Regio-isomers <i>int.</i>				Regio-isomers <i>ext.</i>				Expl. ^a [pm-IN] _{int} S=1/2
	Dd5 S=1/2	Dd5* S=3/2	Td5 S=1	Td5** S=2	Dd6 S=1/2	Dd6* S=3/2	Td6* S=1	Td6* S=2	
$dC9^{An}-C1^{Pm}$	1.484	1.442	1.487	1.439	1.485	1.469	1.485	1.472	1.477 1.394 1.280 1.504 1.551 1.492 1.268 19.1
$dC4^{Pm}-C2^{IN}$	1.464	1.451	1.465	1.453	1.480	1.478	1.481	1.479	
$dC2^{IN}-N1^{IN}$	1.414	1.414	1.414	1.414	1.409	1.410	1.409	1.410	
$dC2^{IN}-N3^{IN}$	1.310	1.319	1.310	1.318	1.300	1.301	1.300	1.301	
$dN3^{IN}-C4^{IN}$	1.487	1.486	1.487	1.486	1.495	1.494	1.495	1.495	
$dC4^{IN}-C5^{IN}$	1.546	1.545	1.546	1.545	1.548	1.548	1.548	1.548	
$dC5^{IN}-N1^{IN}$	1.485	1.483	1.485	1.484	1.485	1.485	1.485	1.485	
$dN1^{IN}-O^{IN}$	1.304	1.305	1.304	1.305	1.302	1.302	1.303	1.302	
θ_1	51.7	(11.6)	59.3	(0.4)	70.2	56.4	72.3	59.1	
θ_2	2.9	0.0	2.6	1.2	62.4	58.1	63.3	59.7	
$\varphi = 180 - \varphi'$	(0)	75.4	(0)	81.5	(0)	(0)	(0)	(0)	
α_1 / α_2	(0)	26.8	(0)	27.5	(0)	(0)	(0)	(0)	
$dC9^{An}-C10^{An} / r$	2.834	2.858	2.849	2.831	2.833	2.856	2.853	2.883	

^a From X-ray structure of 2-(5-pyrimidinyl)-4,4,5,5-tetramethyl-4,5-dihydro-1H-imidazol-1-oxyl.^[1]

Table SI-II. Selected structural parameters computed for oxoverdazyl (OV) based dyads (**Dd7**, **Dd8**) and triads (**Td7**, **Td8**) in both the ground and the excited (*) states. Distances in Å, angles in degrees. For labeling scheme refer to Figures 1, 2 and 3.

	Regio-isomers <i>int.</i>				Regio-isomers <i>ext.</i>			
	Dd7 S=1/2	Dd7* S=3/2	Td7 S=1	Td7* S=2	Dd8 S=1/2	Dd8* S=3/2	Td8 S=1	Td8* S=2
$dC9^{An}-C1^{Pm}$	1.485	1.438	1.487	1.437	1.484	1.463	1.485	1.465
$dC4^{Pm}-C1^{OV}$	1.470	1.455	1.470	1.458	1.484	1.480	1.484	1.480
$dC1^{OV}-N2^{OV}$	1.352	1.358	1.352	1.358	1.350	1.354	1.350	1.354
$dN2^{OV}-N3^{OV}$	1.377	1.378	1.377	1.378	1.381	1.379	1.381	1.380
$dN3^{OV}-C4^{OV}$	1.397	1.396	1.397	1.396	1.395	1.395	1.395	1.395
$dC4^{OV}-O^{OV}$	1.246	1.247	1.246	1.247	1.247	1.247	1.247	1.247
$dN3^{OV}-R^{OV}$	1.460	1.460	1.460	1.460	1.460	1.460	1.460	1.460
$a(N6^{OV}C1^{OV}N2^{OV})$	126.1	125.8	126.1	125.8	127.0	126.4	127.0	126.5
θ_1	53.4	(1.6)	60.7	(2.4)	70.5	52.9	73.5	54.3
θ_2	0.3	0.1	0.6	0.7	39.8	0.4	40.3	11.5
$\varphi = 180 - \varphi'$	(0)	77.8	(0)	80.5	(0)	(0)	(0)	(0)
α_1 / α_2	(0)	28.6	(0)	28.0	(0)	(0)	(0)	(0)
$dC9^{An}-C10^{An} / r^a$	2.834	2.854	2.847	2.834	2.835	2.861	2.862	2.894

Table SI-III. Selected structural parameters computed for verdazyl derivatives **HTd71** and **HTd72** in the ground and excited (*) states. Distances in Å, angles in degrees. For labeling scheme refer to Figures 2 and 3.

	HTd71	HTd71*	HTd72	HTd72*
	S=1/2	S=3/2	S=1/2	S=3/2
$dC10^{An}-C1^{Pm/Ph}$	1.490	1.448	1.494	1.486
$dC9^{An}-C1^{Pm}$	1.487	1.436	1.486	1.438
$dC4^{Pm}-C1^{OV}$	1.470	1.457 ₅	1.470	1.455
$dC1^{OV}-N2^{OV}$	1.352	1.357	1.352	1.358 ₅
$dN2^{OV}-N3^{OV}$	1.377	1.377 ₅	1.377	1.378
$dN3^{OV}-C4^{OV}$	1.397	1.396	1.397	1.396
$dC4^{OV}-O^{OV}$	1.246	1.247	1.246	1.247
θ_1 (pm/ph)	62.7	(0.8)	77.0	64.5
θ_1 (OV)	57.4	(0.7)	56.4	(0.7)
θ_2 (OV)	2.1	0.0	0.6	0.0 ₅
$\varphi = 180 - \varphi'$	(0)	82.1	(0)	<i>npd</i> ^a
α_1 / α_2	(0)	30.0	(0)	27.5
$dC9^{An}-C10^{An} / r$	2.850	2.828	2.859	2.873

^a *npd*: not properly defined.

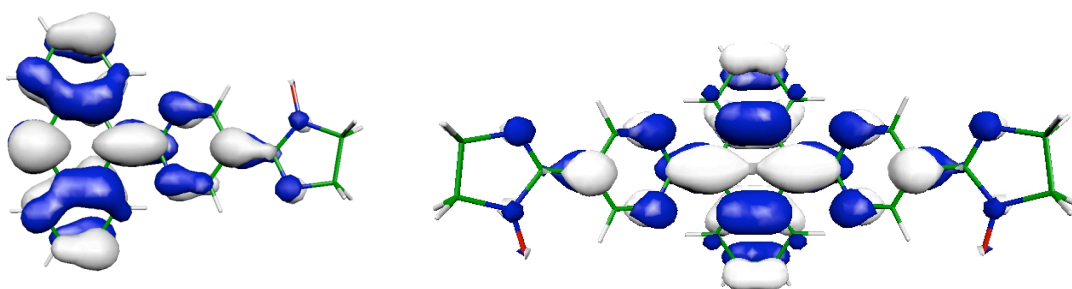


Figure SI-I. Highest singly occupied MO (SOMO) of **Dd5*** and **Td5*** species (contour value 0.025 a.u.).

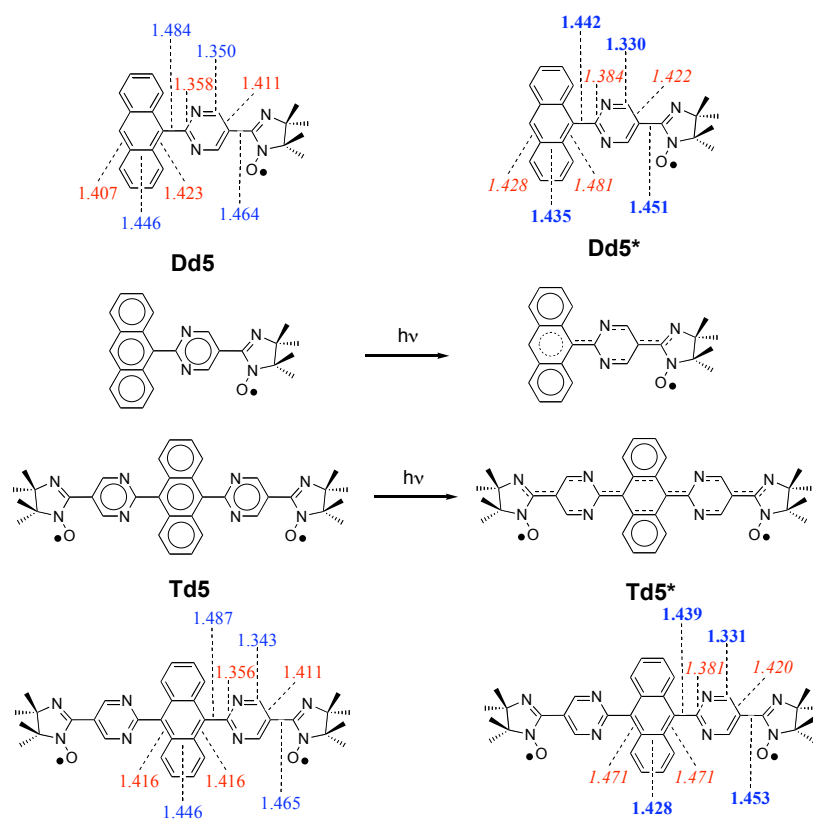


Figure SI-II. Selected bond lengths (in Å) computed for **Dd5** and **Td5** species at the ground and the excited state. Values in blue **[boldface]** (red *[italic]*) correspond to a **shortening** (*elongation*) of bonds when going from the ground to the lowest THEXI state, respectively. Pictorial representations illustrate salient electronic changes (circles refer to aromatic character of the various rings).

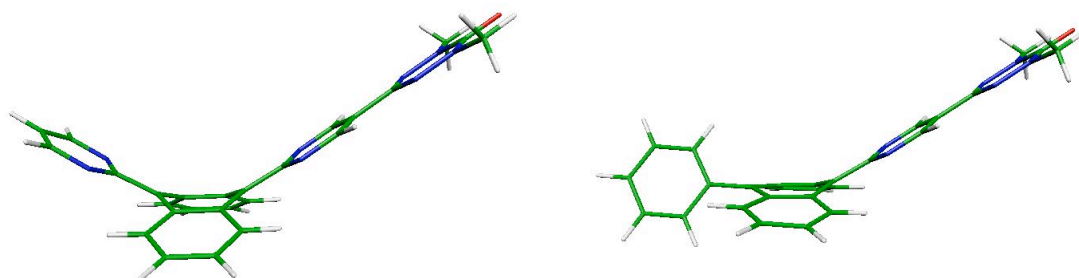


Figure SI-III. Optimized excited-state structures of **HTd71*** and **HTd72*** species.

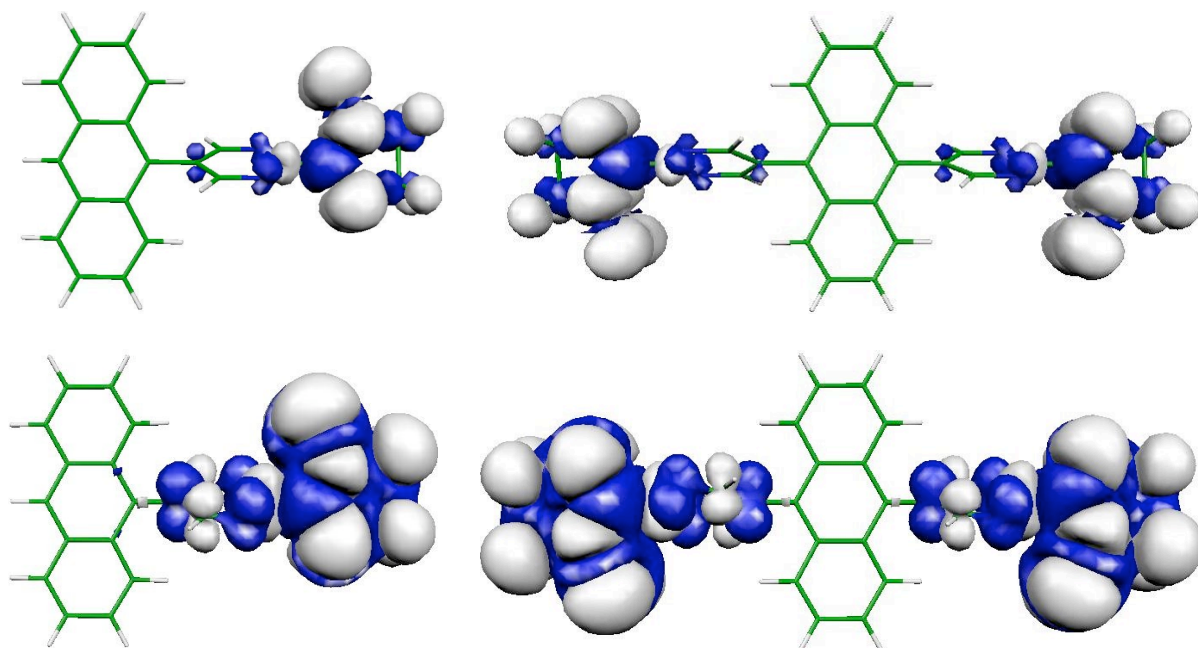


Figure SI-IV. Spin density patterns computed for **Dd6** and **Td6**. $S = 1/2$ and $S = 1$; contour 5×10^{-4} au. (top) value 5×10^{-5} au (bottom).

Table SI-IV. Calculated Mülliken charge differences^[2] (Δe , in 10^{-3} electron units, e.u.) between the lowest THEXI state (LTS) and the ground state (GS) of various PMMDs and reference species. Data are given for individual An (P), pm/ph (B) and OV/IN (SC) building blocks, with $\Delta e(P) + \Delta e(B) + \Delta e(SC) = 0$. Negative Δe value indicates reduction of the component in the LTS compared to GS.

Δe	Regio-isomers <i>int.</i>							Regio-isomers <i>ext.</i>				
	Ref5 ^a	Dd5	Dd7	Td5	Td7	HTd71	HTd72	Ref6	Dd6	Dd8	Td6	Td8
P	-24	+73	+90	+30	+38	+64	+38	+23	+28	+42	+47	+99
B	+12	-49	-62	+1	-1	-32 ^b (-13 ^c)	-21 ^b (+8 ^d)	-11.5	-23	-42	-20	-50
SC		-24	-28	-16	-18	-19	-25	-5	0.0	-3.5	+0.5	

^a LTS is saddle-shaped distorted. In the case of an hypothetical axially distorted LTS, charge variations are the following: : P ($\Delta e = -15 \times 10^{-3}$ e.u.) and B ($\Delta e = +7.5 \times 10^{-3}$ e.u.). ^b B element connecting the An core and the unique remote SC (OV). ^c Dangling pyrimidinyl. ^d Dangling phenyl.

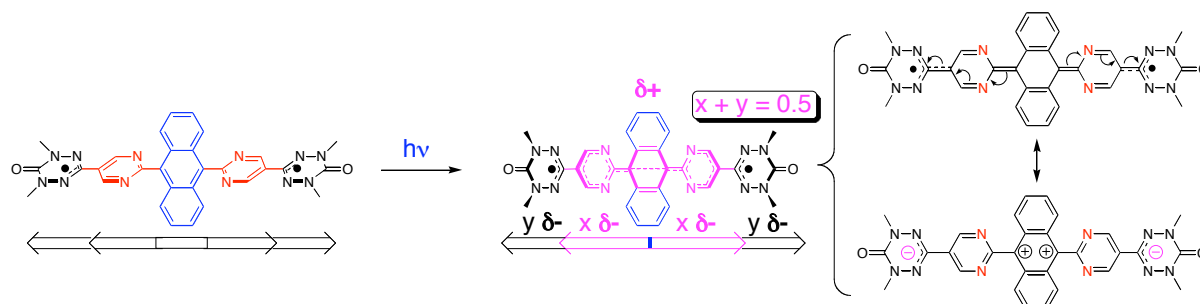


Figure SI-V. Arrows indicate polarization direction of various functional elements at the electronic level and partial ICT in the excited state; relevant canonical forms accounting for the partial reduction of dangling SC acceptors in the case of the saddle-shaped distorted LTS of regio-isomer *int.*

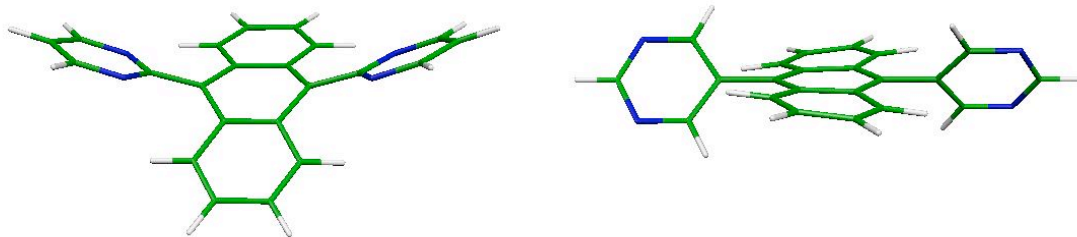


Figure SI-VI. Optimized structures of mono-reduced **Ref5** and **Ref6** species.

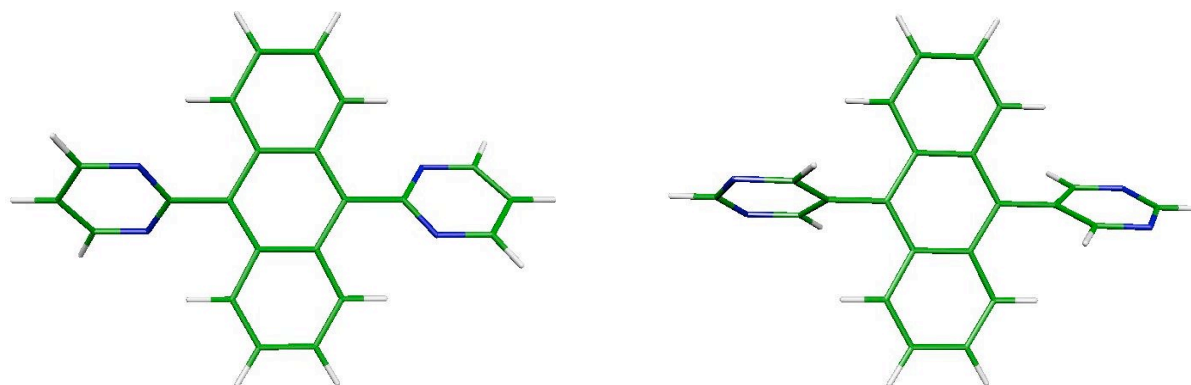


Figure SI-VII. Optimized structures of mono-oxidized **Ref5** and **Ref6** species.

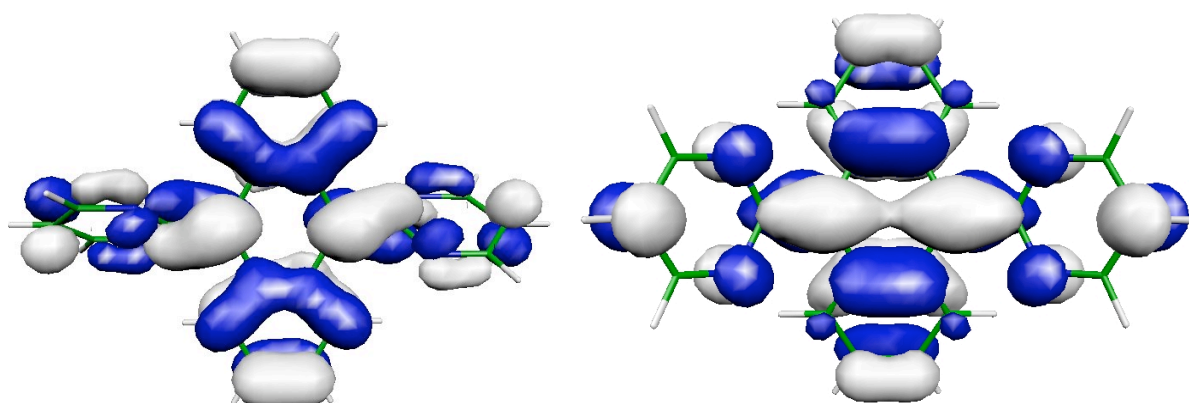


Figure SI-VIII. Highest singly occupied MO (SOMO) of **Ref5*** axially distorted (left) and saddle-shaped distorted (right); contour value 0.025 a.u.

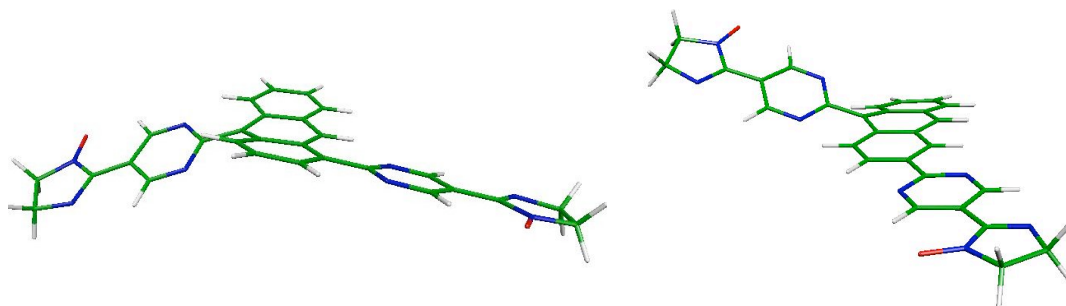


Figure SI-IX. Optimized geometries of the **Td3bis*** and **Td4bis*** triads in their lowest (quintet) THEXI states.

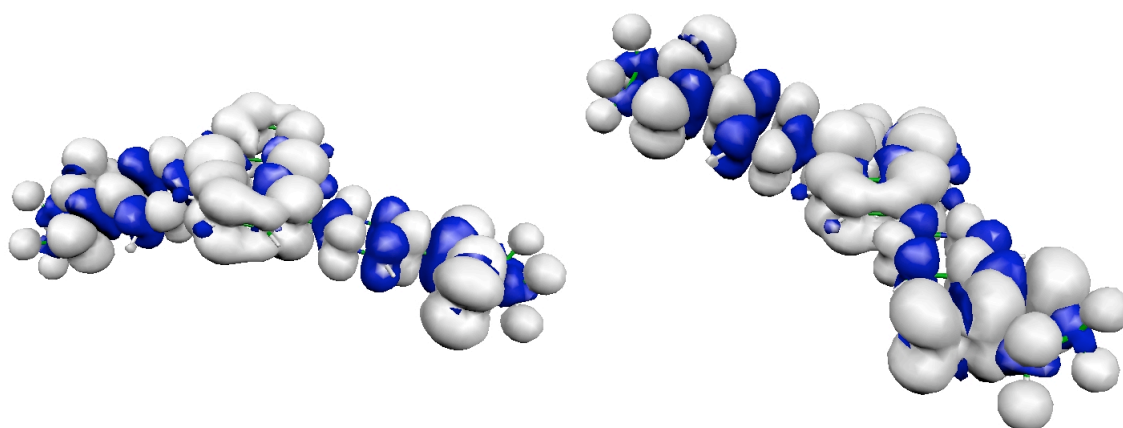


Figure SI-X. Spin density patterns computed for **Td3bis*** and **Td4bis*** triads in their lowest (quintet) THEXI; contour value 5×10^{-4} au.

References.

- [1] F. Lanfranc de Panthou, D. Luneau, J. Laugier, P. Rey, *J. Am. Chem. Soc.* **1993**, *115*, 9095–9100.
- [2] Aware of the possible bias of discussing absolute values of Mulliken charges as well as for clarity and consistency with ASP (that is, to avoid other charge analysis), we comment only on their variation on passing from the ground state to the LTS.